PHILOSOPHICAL TRANSACTIONS OF THE ROYAL SOCIETY A MATHEMATICAL, PHYSICAL & ENGINEERING SCIENCES

The Fermi Surfaces of Copper, Silver and Gold II. Calculation of the Fermi Surfaces

D. J. Roaf

Phil. Trans. R. Soc. Lond. A 1962 **255**, 135-152
doi: 10.1098/rsta.1962.0012

THE FERMI SURFACES OF COPPER, SILVER AND GOLD
II. CALCULATION OF THE FERMI SURFACES

By D. J. ROAF
Cavendish Laboratory, University of Cambridge and
Clarendon Laboratory, University of Oxford

(*Communicated by D. Shoenberg, F.R.S.—Received* 12 *March* 1962)

CONTENTS

	PAGE		PAGE
Introduction	135	References	148
Choice of analytic representation	136	Appendix. Numerical calculations	149
Fitting the de Haas–van Alphen data	137	Details of integration	149
Use of the anomalous skin effect	139	Accuracy	151
Radius vectors	141	Fitting procedure	151
Variation of area with k_H	143	Further comments on the computer program	152
Cyclotron resonance	144		

Fermi surfaces, similar in shape to that proposed for copper by Pippard, have been computed which fit Shoenberg's experimental measurements of the de Haas–van Alphen effect in copper, silver and gold. It is shown that these are reasonably consistent with other experimental results, particularly the anomalous skin measurements of Pippard and Morton, although the shapes of the surfaces are markedly different in detail from the surfaces proposed by Pippard and Morton. Consideration has been given to using the cyclotron resonance data of Kip, Langenberg & Moore to deduce electron velocities, but without success.

Introduction

In the course of a general investigation of the possibility of calculating various metal properties from an analytically specified Fermi surface, Shoenberg's results (see preceding paper, referred to subsequently as I) on the de Haas–van Alphen effect in copper, silver, and gold became available. It was decided, as a first step, to apply the computer programs already being worked out to the specific problem of fitting a Fermi surface to each of these metals on the basis of de Haas–van Alphen data alone. From the surfaces obtained, other properties of the metals can be computed: the anomalous skin effect, the frequency of magneto-acoustic oscillations, and, with certain assumptions about velocities and relaxation times, the cyclotron masses and the magneto-resistance. Indeed, it should be possible to use experimental data on cyclotron resonance and magneto-resistance to deduce the electronic velocities and relaxation times at each point on the Fermi surface.

So far, only a part of this program has been carried out; first Fermi surfaces have been computed which, within experimental error, fit all Shoenberg's data on the frequencies of de Haas–van Alphen oscillations for different directions of the magnetic field. The anomalous skin effect for copper and silver was then computed for these surfaces, and was

found to have the same general character as the experimental results (Pippard 1957; Morton 1960), but there were large discrepancies in detail. The anomalous skin effect is, however, particularly sensitive to local regions of low curvature on the Fermi surface, and it was found possible, without seriously upsetting the fit with the de Haas–van Alphen data, to modify the Fermi surfaces slightly in such a way that the agreement with the anomalous skin effect data was considerably improved. This is the first demonstration that the same Fermi surface can account for two such different phenomena as the de Haas–van Alphen effect and the anomalous skin effect. The surfaces obtained are also reasonably consistent with data on magneto-acoustic oscillations (Bohm & Easterling 1962; Morse, Myers & Walker 1961, and private communication) and with recent band-structure calculations (Segall 1962; Burdick 1961).

Consideration has been given to using the cyclotron resonance data of Kip, Langenberg & Moore (1961) for computing electron velocities but, as explained below, this has not proved possible. As a result of this and a shortage of computing time, very little has been done on magneto-resistance; but the topology of the computed surfaces is, of course, consistent with the experimental data of Alekseevski & Gaidukov (1959), as has been already pointed out by Priestley (1960).

Choice of analytic representation

Segall (1962) and Burdick (1961) have recently calculated band-structures for copper, based on particular assumptions about the potential in the metal and on various computational assumptions. In principle, it should be possible to vary these assumptions to make the Fermi surface fit the experimental data, such as the de Haas–van Alphen frequencies. In practice, however, this would be exceedingly difficult because these Fermi surfaces are described arithmetically rather than analytically, and for each trial assumption the whole computation would have to be repeated. All that can be done easily at present is to compare the Fermi surfaces resulting from the particular assumptions of Segall and Burdick with the Fermi surface which has been fitted to the de Haas–van Alphen and anomalous skin effect data (see table 3) below.

Ziman (1961) and Cornwell (1961) have used the 'nearly-free electron' band-structure approximation. This finds the energy at a point $\mathbf{k}$ by reflecting the point in the neighbouring zone-faces, and evaluating a determinant whose size depends on the number of reflexions considered, but the energy surface obtained is not smooth unless a large number of reflexions are used. Cornwell smoothed it by fitting a Fourier series for the energy at 100 points in a forty-eighth of the zone with a least-squares procedure. Ziman, who used only one reflexion, did not require very high accuracy and obtained a surface which was well suited for computation. Ziman's procedure is, however, not accurate enough for fitting the de Haas–van Alphen effect; indeed, although Ziman's surface is most accurate near the necks, the detailed surface here for gold does not agree as well with experiment as the surfaces discussed in his paper.

The Fourier expansion used by Cornwell had been used by García Moliner (1958), and Hume-Rothery & Roaf (1961) to fit experimental data and is formally the same as the tight-binding approximation of Slater & Koster (1954). It has also been used by J. R. Anderson (private communication) to fit Gold's (1958) experimental de Haas–van Alphen data

in lead. In principle, given enough terms the true energy band-structure should be obtained, since the correct symmetry is built in, but since computational difficulties increase with the number of terms, it was decided to use at most six terms. We shall, therefore, consider Fermi surfaces of the form:

$$\begin{aligned} W_F = W(\mathbf{k}) = {} & 3 - \cos\tfrac{1}{2}ak_y \cos\tfrac{1}{2}ak_z - \cos\tfrac{1}{2}ak_z \cos\tfrac{1}{2}ak_x - \cos\tfrac{1}{2}ak_x \cos\tfrac{1}{2}ak_y \\ & + C_{200}(3 - \cos ak_x - \cos ak_y - \cos ak_z) \\ & + C_{211}(3 - \cos ak_x \cos\tfrac{1}{2}ak_y \cos\tfrac{1}{2}ak_z - \ldots) \\ & + C_{220}(3 - \cos ak_y \cos ak_z - \ldots) \\ & + C_{310}(6 - \cos\tfrac{3}{2}ak_x \cos\tfrac{1}{2}ak_y - \cos\tfrac{3}{2}ak_x \cos\tfrac{1}{2}ak_z - \ldots) \\ & + C_{321}(6 - \cos\tfrac{3}{2}ak_x \cos ak_y \cos\tfrac{1}{2}ak_z - \ldots), \end{aligned} \tag{1}$$

where a is the lattice constant (see I, table 2).

It should be emphasized that (1) is merely a convenient implicit equation for the Fermi surface; thus $W(\mathbf{k})$ is not the band-structure and W_F is not the Fermi energy.

Fitting the de Haas–van Alphen data

In the experimental curves of belly frequency variation (see I, figures 7, 8, and 10), the quantity actually measured is a beat frequency, i.e. a frequency *difference*, and this is most accurately determined where it is a maximum or minimum. It will be seen from the

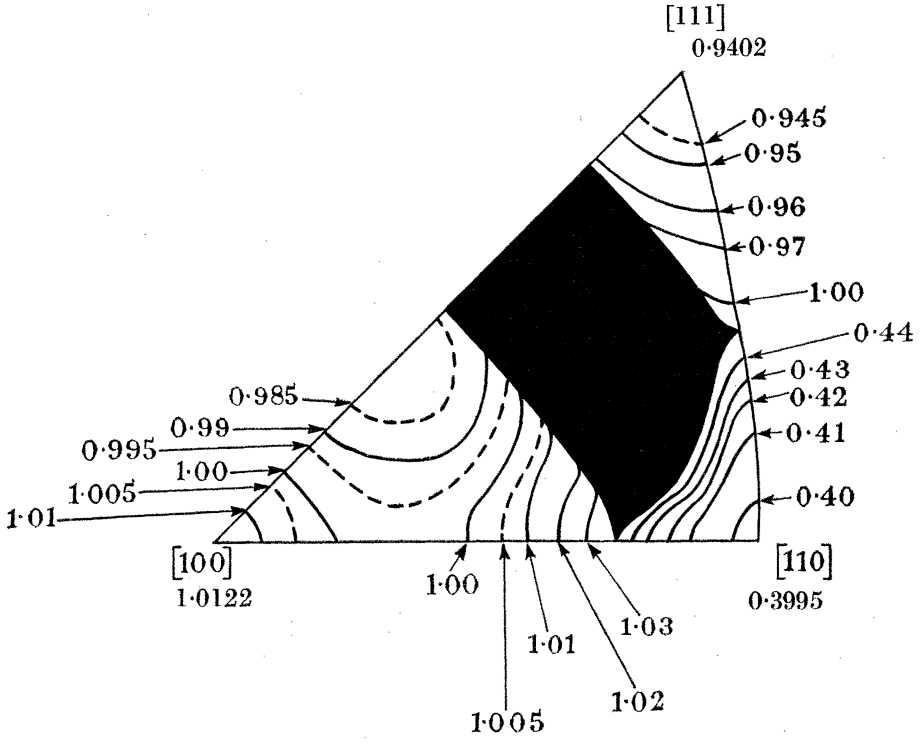

Figure 1. Approximate contours of central cross-sectional area for suggested gold surface (Au v). The values are taken from table 5. The shaded portion contains extended orbits.

contour diagram of central cross-sectional area against direction (figure 1) that the maxima and minima are stationary points for all traverses through the points, so that errors of a degree or so in the mounting of the specimens will not be very serious.

For each metal the differences available are those between the [100] frequency, F_{100}, the frequency minima near [100] in the (011) and (001) traverses, F_{m1} and F_{m2}, and the [111] frequency, F_{111}. The other important imformation available for determining the surface is the neck frequency, $F_{111}(N)$. All these were used in the reduced dimensionless form

$$D = (F_{100}-F_{111})/F_s, \quad D_1 = (F_{100}-F_{m1})/F_s, \quad D_2 = (F_{100}-F_{m2})/F_s,$$
$$N = F_{111}(N)/F_s \quad \text{(I, equation (8))}, \qquad (2)$$

where F_s is the frequency for a spherical Fermi surface, containing one electron per atom (see I, equation (7) and table 2).

Preliminary investigation suggested that a four-term theoretical surface (with $C_{211} = C_{321} = 0$), which agreed with the experimental values of D, D_1, D_2, and N, would give a fair fit elsewhere. However, it is still necessary to determine the absolute size of the belly of the surface. This could be done from the absolute experimental frequency values, or from the theoretical assumption that the conduction band contains exactly one electron per atom; i.e. that the Fermi surface occupies half the Brillouin zone. At the time the fitting was started, Shoenberg's absolute values of frequencies were somewhat discrepant with this assumption, but, as explained in I (p. 95), this proved to be due to a calibration error, and there is now no reason to suppose that the volume is different from half the zone volume. Since the absolute values are still subject to errors of order 1 or 2%, it was thought best to retain the precise volume (half the zone), rather than fit the experimental absolute values.

TABLE 1

	coefficients in the expansion (1)						fitting data from equation (2)				surface	
	W_F	C_{200}	C_{211}	C_{220}	C_{310}	C_{321}	D	D_1	D_2	N	area	volume
GM.	3·6301	0·0995	0	0	0	0	−0·0134	no dip	no dip	0·0182	0·997	1·0071
HR.R.	3·84	0·119	0	0·064	0	0	0·0240	0·0046	0·0023	0·043	0·964	0·9813
Cu IV	3·8555	0·1234	0	0·0547	0·0015	0	0·0307	0·0062	0·0031	0·0402	0·976	1·0002
Cu VI	3·5531	0·1152	−0·05	0·0429	0·0435	−0·05	0·0306	0·0062	0·0037	0·0402	0·971	1·0002
expt. Cu	—	—	—	—	—	—	0·0305	0·0062	0·0035	0·0402	—	—
Ag IV	3·7362	0·1267	0	0·0263	−0·011	0	0·0281	0·0064	0·0033	0·0187	0·999	1·0001
Ag VI	3·4343	0·1105	−0·05	0·0116	−0·065	0·04	0·0285	0·0067	0·0051	0·0188	0·999	1·0005
expt. Ag	—	—	—	—	—	—	0·0286	0·0067	0·004	0·0188	—	—
Au IV	3·8777	0·1410	0	0·0606	−0·0095	0	0·0720	0·0327	0·0166	0·0320	1·005	1·0000
Au V	3·9065	0·1396	0	0·0593	−0·02	0·015	0·0720	0·0307	0·0161	0·0313	1·006	1·0002
expt. Au	—	—	—	—	—	—	0·0722	0·0309	0·0162	0·0313	—	—

GM. is the surface proposed by García Moliner (1958) to describe Pippard's (1957) theoretical surface. HR.R. is a surface used by Hume-Rothery & Roaf (1961), which fitted Shoenberg's preliminary results. The surface areas and volumes are expressed as ratios of those of the Fermi sphere.

However, if we include this assumption, we cannot rely on fitting more than three out of D, D_1, D_2, and N, with a four-term surface. It was decided to use D, D_1,* and N, as the basic data for fitting in the first place, and then to use the remaining data (i.e. D_2 and the other points on the experimental curves, as well as other features, such as the rosette and dog's bone frequencies and their angular variations and the angular variation of the neck frequency) as checks on the validity of the formula obtained. The procedure, by which the best values of W_F, C_{200}, C_{220}, and C_{310} are determined by the volume assumption and the experimental data, is described in the appendix. The best four-term surfaces (Cu IV, Ag IV, and Au IV) are specified in table 1 and, as is shown in figures 7, 8 and 10,

* In gold, however, D_2 was used because this value was the only one available at the time.

and tables 3 to 6 of I, they fit the experimental data, on the whole, remarkably well. For gold, however, where D_2 was fitted instead of D_1 in the first place, and where the anisotropy is much greater than in copper and silver, there is an appreciable discrepancy between the calculated and experimental values of D_1 (see I, figure 10), and a modified surface (Au v) with a fifth term was calculated to eliminate this discrepancy.

Use of anomalous skin effect

A program was set up to compute the anomalous skin effect (see appendix), with the use of the formula developed by Morton (1960, p. 64), which is essentially an improved version of Pippard's 'ineffectiveness concept'. This was first used on surfaces proposed by Pippard (1957) and Morton and the results obtained, shown in table 2 as P. I and M.,

Table 2. Anomalous skin effect for a (110) traverse

	R_x						R_y
angle from [001]	0°	22°	45°	54·7°	62°	90°	90°
GM.	274	350	345	338	303	370	395
HR.R.	248	375	314	343	277	403	389
Cu IV	245	379	304	337	267	398	379
Cu VI	226	(374)	332	338	304	410	394
P. I	244	(363)	(331)	312	—	375	367
P. II	241	388	342	(341)	277	408	391
expt. Cu	236	402	327	(345)	285	417	382
angle from [001]	0°	20°	46°	54·7°	65°	90°	90°
Ag IV	268	368	320	327	263	404	383
Ag VI	292	352	(317)	336	(275)	383	384
M.	284	351	330	318	289	372	372
expt. Ag	282	360	325	328	279	356	347
angle from [001]	0°	20°	40°	54·7°	60°	90°	90°
Au V	247	382	331	281	260	429	364

The values in brackets are estimates from curves through nearby points. The experimental results, taken from Pippard (1957) (Cu) and Morton (1960) (Ag) are scaled arbitrarily and corrected for polarization (Morton, p. 91) by increasing the difference between R_x and R_y by 5%; P. II (Pippard's final surface, which has no analytic representation), whose values were computed by Pippard, was scaled in the same way as the experimental points of copper. The other theoretical values have been scaled so that lattice size is immaterial. P. I is a preliminary trial surface used by Pippard (with $A = 0{\cdot}3$, $B = -5{\cdot}6$, and $C = 0$)

$$1 = x^2+y^2+z^2+A(y^2z^2+z^2x^2+x^2y^2)+Bx^2y^2z^2+C(y^4z^4+z^4x^4+x^4y^4).$$

M. is Morton's final surface ($A = 0{\cdot}467$, $B = -5{\cdot}35$, and $C = -0{\cdot}86$). In this expression x, y, z represent k_x, k_y, k_z and the surface is scaled to contain one electron per atom. The other surfaces are described in table 1.

were indeed almost identical with those of their own calculations. Pippard's final surface, P. II, was not in analytic form, but García Moliner (1958) had shown that a two-term Fourier expansion, GM., would fit Pippard's radius vectors to 1%. The anomalous skin effect was calculated for this surface, GM., also and for a surface, HR.R., used by Hume-Rothery & Roaf (1961). Although the differences between the radius vectors of GM. and those of P. II were small, the differences in the computed anomalous skin effect were large, and the agreement with the experimental data was far worse for GM. than for P. II. The HR.R. surface, which is a three-term Fourier expansion to fit Shoenberg's preliminary results, gave a much better fit than GM., though not as good a fit as P. II.

When the four-term surfaces, Cu IV and Ag IV, became available, the anomalous skin effect was calculated for them too. The results of all these calculations are given in table 2. It can be seen that there are still considerable discrepancies in detail, although they reproduce the qualitative form of the experimental data.

It was found possible to choose non-zero values of C_{211} and C_{321} (readjusting the values of the other coefficients to avoid spoiling the fit to D, D_1, N, and the volume), which

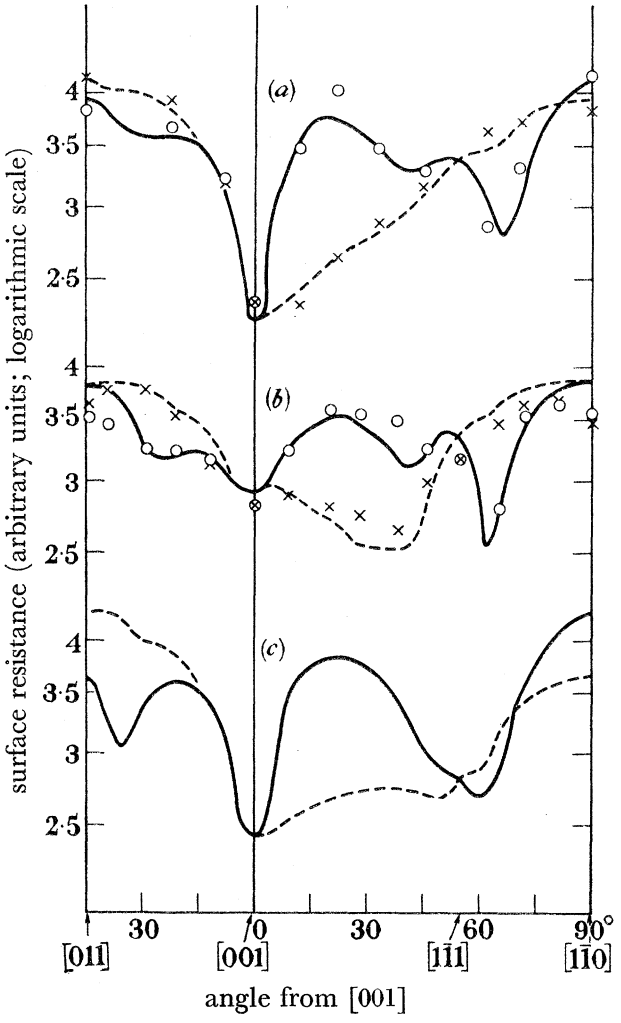

FIGURE 2. Anomalous skin effect surface resistance as a function of angle for (*a*) copper (Cu VI), (*b*) silver (Ag VI), and (*c*) gold (Au V). The left-hand portion of each curve is between [011] and [001] in a (100) plane; the right-hand portion is between [001] and [1$\bar{1}$0] in a (110) plane. ——, R_x; – – –, R_y (theory). ○, R_x; ×, R_y (experiment—(*a*) Pippard 1957, (*b*) Morton 1960). The experimental points are scaled arbitrarily.

greatly improved the agreement with the anomalous skin effect, and the resulting surfaces (Cu VI and Ag VI) are described in table 1 and their anomalous skin effects are given in table 2 and figure 2. The agreement with the experimental points for copper is nearly as good as that found by Pippard for his final (non-analytic) surface, P. II. For silver the agreement is not so good as the fit of the surface, M., which Morton proposed to fit his data. However, Morton's surface does not make contact with the Brillouin zone, and is, therefore, incompatible with the evidence of the de Haas–van Alphen data, though it should

be added that Morton did not put much reliance on his conclusion that there was no contact, but in any case, the variations of belly area with angle for both Morton's surface, M., and Pippard's final surface, P. II, are quite incompatible with Shoenberg's de Haas–van Alphen data. More terms are needed in the expansion to 'trim' the silver surface; moreover, as can be seen from figure 8 of I, Ag VI does not fit the de Haas–van Alphen data quite as well as Ag IV. Unfortunately without a major change in programming it is not possible to investigate the consequence of using more terms.

The anomalous skin effect has not yet been measured in gold, so only the computed effect (for Au V) is shown in figure 2. Judging by the discrepancies between the experimental data and the computed anomalous skin effect for Cu IV and Ag IV, it is likely that the anomalous skin effect computed for gold will prove to be no more than a guide within, say, 15 or 20% of the true curve.

Anomalous skin effect measurements on polycrystalline specimens should give estimates of the total surface area of the Fermi surface (Chambers 1952). The computed areas for the surfaces discussed here are given in table 1, and it can be seen that they are almost exactly the same as the area of a free electron Fermi sphere of the same volume. Chambers's experimental value for copper (1·00) agrees well, but his values for silver (0·72) and gold (0·71) are discordant with the computed values. As is pointed out by Chambers the discrepancies are probably due to the specimen surfaces being too rough.

Radius vectors

Although the de Haas–van Alphen effect can scarcely discriminate between the four- and six-term surfaces, there are appreciable differences in the radius vectors, as can be seen in table 3, and even larger differences between these and the surfaces based on the

Table 3. Radius vectors in units of k_s, the radius of the Fermi sphere, as functions of polar angles

	(110) traverse								(100) traverse		
angle from [001]	0°	15°	30°	45°	54·7	60°	75°	90°	15°	30°	neck radius
Cu IV	1·065	1·005	0·985	contact	contact	contact	0·986	0·945	1·002	0·955	0·201*
Cu VI	1·076	1·006	0·984	contact	contact	contact	0·985	0·943	0·998	0·945	0·200*
P. II	1·00	0·995	0·995	1·07	contact	contact	1·00	0·965	0·99	0·97	0·157+
M.M.W. Cu	1·03	—	—	—	contact	contact	0·99	0·96	—	—	0·18+
B.E. Cu	1·036	—	—	contact	contact	contact	0·998	0·956	0·992	—	0·195+
B.	1·05	—	—	—	contact	contact	—	0·96	—	—	0·18*
											0·16+
S.	1·02	1·00	0·99	contact	contact	contact	0·99	0·95	—	—	0·21+
Ag IV	1·052	1·008	0·990	1·060	contact	contact	0·990	0·962	1·006	0·970	0·137*
Ag VI	1·029	1·004	0·987	1·057	contact	contact	0·989	0·965	1·008	0·979	0·137*
M.	1·006	0·995	0·997	1·047	1·081	1·068	1·000	0·975	0·994	0·979	None
B.E. Ag	1·072	—	—	1·037	contact	contact	0·982	0·955	0·979	0·911	0·142+
Au IV	1·140	1·020	0·982	1·090	contact	contact	0·980	0·943	1·016	0·954	0·179*
Au V	1·129	1·021	0·984	1·092	contact	contact	0·981	0·945	1·020	0·959	0·177*
M.M.W. Au	1·12	—	—	—	contact	contact	0·99	0·93	—	—	0·19+
B.E. Au	1·068	—	—	—	contact	contact	0·982	0·930	1·016	0·916	0·180+

* Measured towards a corner of the zone. + Measured towards the middle of an edge. (The difference between these two measurements must be small, since the average neck-radius, $\sqrt{N}$, for each theoretical surface is within $\frac{1}{4}$% of the radius towards a corner.) The experimental values from magneto-acoustic oscillations are taken from Morse *et al.* (1961 and private communication) (referred to as M.M.W.) and from Bohm & Easterling (1962) (B.E.). The theoretical values are from Burdick (1961) (B) and Segall (1962 and private communication) (S). The other surfaces are explained in tables 1 and 2.

anomalous skin effect by Pippard (1957) and Morton (1960) for copper and silver (P. II and M.), although the differences in the anomalous skin effect between, say, Cu VI and P. II are not at all large. This shows that, though a good approximation to the Fermi surface can be obtained from the de Haas–van Alphen data alone, extremely high experimental accuracy is required before the surface can be determined to better than 1% in radius vector. With the accuracy obtained in I, however, the uncertainty in the determination of the Fermi surface can be considerably reduced by using the anomalous skin data. Pippard's experience in fitting his own surface suggests that it is unlikely that the addition of further extra terms to $W(\mathbf{k})$ to improve the anomalous skin effect fit still further will change the radius vectors by more than $\frac{1}{4}$% for copper or 1% for silver.

TABLE 4. RADIUS VECTORS OF THE FINAL SURFACES, IN UNITS OF k_s, AS FUNCTIONS OF POLAR ANGLES

	Cu VI				Ag VI				Au V			
θ \ ϕ	0°	15°	30°	45°	0°	15°	30°	45°	0°	15°	30°	45°
0°	1·076	1·076	1·076	1·076	1·029	1·029	1·029	1·029	1·129	1·129	1·129	1·129
5°	1·061	1·061	1·061	1·061	1·026	1·026	1·026	1·026	1·103	1·103	1·103	1·103
10°	1·030	1·031	1·032	1·033	1·018	1·018	1·017	1·017	1·058	1·058	1·058	1·058
15°	0·998	1·000	1·004	1·006	1·008	1·007	1·005	1·004	1·020	1·020	1·021	1·021
20°	0·973	0·976	0·984	0·987	0·998	0·997	0·994	0·993	0·992	0·993	0·995	0·996
25°	0·955	0·960	0·973	0·980	0·989	0·988	0·987	0·986	0·972	0·975	0·981	0·984
30°	0·945	0·953	0·972	0·984	0·979	0·981	0·985	0·987	0·959	0·965	0·977	0·984
35°	0·942	0·953	0·981	1·001	0·972	0·976	0·989	0·997	0·950	0·960	0·982	0·996
40°	0·942	0·957	1·000	1·036	0·967	0·975	0·999	1·018	0·946	0·960	0·996	1·025
45°	0·943	0·963	1·027	contact	0·965	0·976	1·014	1·057	0·945	0·962	1·018	1·092
50°	0·942	0·965	1·055	contact	0·967	0·978	1·029	contact	0·946	0·965	1·039	contact
55°	0·942	0·965	1·064	contact	0·972	0·981	1·033	contact	0·950	0·968	1·046	contact
60°	0·945	0·966	1·047	contact	0·979	0·983	1·025	contact	0·959	0·972	1·034	contact
65°	0·955	0·970	1·021	1·124	0·989	0·984	1·009	1·051	0·972	0·976	1·012	1·076
70°	0·973	0·977	0·995	1·024	0·998	0·986	0·995	1·012	0·992	0·983	0·993	1·014
75°	0·998	0·985	0·973	0·985	1·008	0·991	0·985	0·989	1·020	0·993	0·977	0·981
80°	1·030	0·992	0·958	0·961	1·018	0·997	0·981	0·975	1·058	1·005	0·967	0·960
85°	1·061	0·997	0·948	0·947	1·026	1·005	0·979	0·967	1·103	1·015	0·960	0·948
90°	1·076	0·998	0·945	0·943	1·029	1·008	0·979	0·965	1·129	1·020	0·959	0·945

Table 3 also shows the radius vectors deduced from their experimental results on magneto-acoustic oscillations by Morse *et al.* (1961 and private communication), and by Bohm & Easterling (1962) and the radius vectors given by the band-structure calculations of Segall (1962) and Burdick (1961). In deriving radius vectors from the magneto-acoustic data it is assumed that the period of the oscillations is related to the extremal value of an external 'calliper' diameter of the Fermi surface. Because of the low phase of the oscillations, this assumption may not be sufficiently reliable, and this may be partly responsible for the slight discrepancies in the radius vectors. The detailed form of the surfaces derived from the band-structure calculations of Segall and Burdick depend on the exact assumptions about the potentials inside the unit cell and the approximations made in the computations. Thus the agreement with both magneto-acoustic oscillations and the band-structure calculations is reasonable considering the difficulties in the experiments and calculations. This tends to confirm the hypothesis that at the present level of experimental precision a single Fermi surface can explain all the experimental data.

The radius vectors for the final surfaces are given more fully in table 4, and the (100) and (110) central sections are shown in figure 3; the cross-sectional areas of the surfaces are given in table 5.

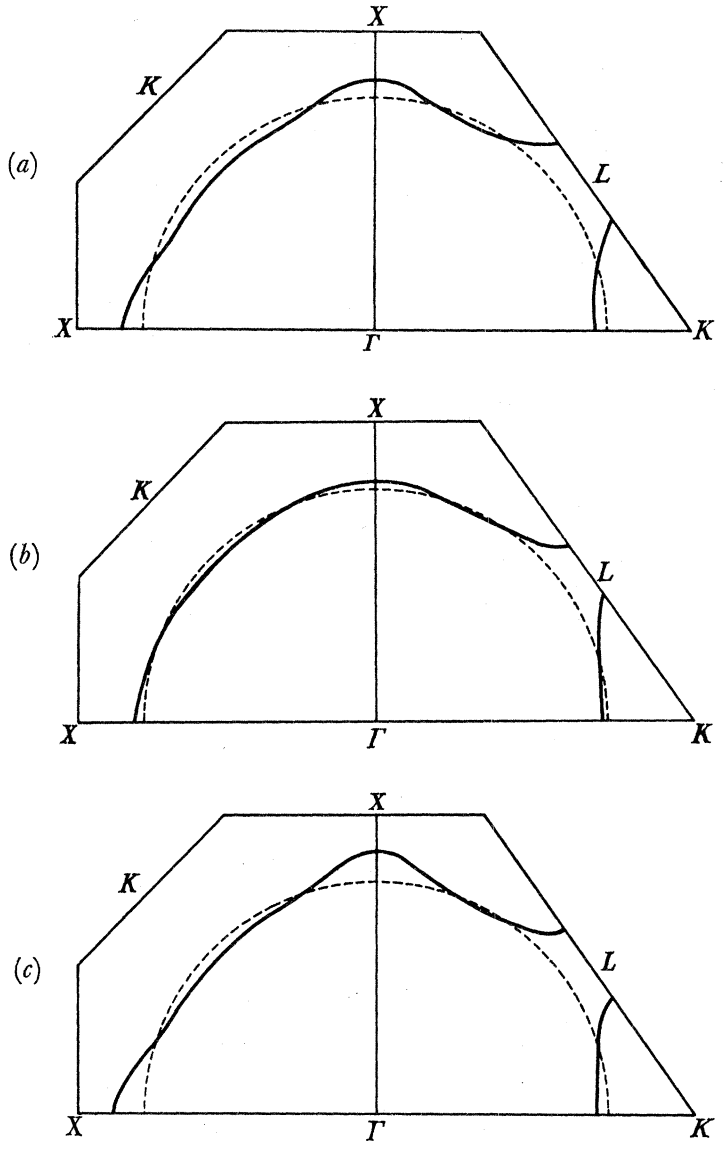

FIGURE 3. Cross-sections of the proposed Fermi surfaces for (*a*) copper (Cu VI), (*b*) silver (Ag VI), and (*c*) gold (Au V). The left-hand portion is a (100) section; the right-hand portion is a (110) section. ——, Theory; – – – –, free electrons.

VARIATION OF AREA WITH k_H

As is pointed out in I, the variation of area with k_H affects the observed amplitude of the de Haas–van Alphen effect. The variation was calculated for several surfaces, but the agreement with experiment was only qualitative (see p. 124 of I). Table 6 shows the variation for Cu VI; the variations for the other surfaces are similar. It will be noticed that the (111) central cross-sectional area is a minimum rather than a maximum with respect to k_H.

TABLE 5. CROSS-SECTIONAL AREAS OF THE FINAL SURFACES, IN UNITS OF A_s ($= \pi k_s^2$, THE CROSS-SECTIONAL AREA OF THE FERMI SPHERE), AS FUNCTIONS OF POLAR ANGLES

central sections

	Cu VI				Ag VI				Au V			
θ \ ϕ	0°	15°	30°	45°	0°	15°	30°	45°	0°	15°	30°	45°
0°	0·9700	0·9700	0·9700	0·9700	0·9905	0·9905	0·9905	0·9905	1·0122	1·0122	1·0122	1·0122
5°	0·9688	0·9688	0·9687	0·9687	0·9891	0·9891	0·9891	0·9891	1·0076	1·0075	1·0073	1·0072
10°	0·9673	0·9669	0·9662	0·9658	0·9866	0·9865	0·9862	0·9861	1·0000	0·9991	0·9974	0·9966
15°	0·9689	0·9675	0·9651	0·9639	0·9855	0·9852	0·9844	0·9840	0·9962	0·9935	0·9888	0·9868
20°	0·9757	0·9728	0·9677	0·9654	0·9880	0·9872	0·9856	0·9848	0·9984	0·9932	0·9850	0·9816
25°	0·9896	0·9848	0·9776	0·9759	0·9948	0·9936	0·9909	0·9895	1·0076	0·9996	0·9882	0·9839
30°	1·0135	*	*	*	1·0065	1·0053	*	*	1·0249	*	*	*
35°	0·4430	*	*	*	1·0247	*	*	*	0·4366	*	*	*
40°	0·4148	*	*	*	0·4331	*	*	*	0·4074	*	*	*
45°	0·4063	*	*	*	0·4246	*	0·9912	0·9752	0·3995	*	*	0·9589
50°	0·4148	*	0·9682	0·9434	0·4331	*	0·9831	0·9651	0·4074	*	0·9685	0·9442
55°	0·4430	*	*	0·9394	1·0247	*	0·9822	0·9620	0·4366	*	0·9696	0·9402
60°	1·0135	*	*	0·9440	1·0065	*	*	0·9657	1·0249	*	*	0·9450
65°	0·9896	*	*	0·9575	0·9948	0·9998	*	0·9758	1·0076	*	*	0·9583
70°	0·9757	0·9755	*	0·9819	0·9880	0·9898	*	0·9914	0·9984	0·9854	*	0·9809
75°	0·9689	0·9665	*	0·4491	0·9855	0·9854	*	1·0114	0·9962	0·9813	*	0·4444
80°	0·9673	0·9652	*	0·4236	0·9866	0·9844	*	0·4431	1·0000	0·9845	*	0·4166
85°	0·9688	0·9673	*	0·4104	0·9891	0·9850	1·0071	0·4288	1·0076	0·9917	1·0227	0·4025
90°	0·9700	0·9689	1·0135	0·4063	0·9905	0·9855	1·0065	0·4246	1·0122	0·9962	1·0249	0·3995

non-central sections

	polar angles				
	θ	ϕ	Cu VI	Ag VI	Au V
			four-cornered rosette		
[100]	0	0	0·4042	0·4084	0·4134
	3	0	0·4067	0·4113	0·4159
	6	0	0·4151	0·4208	0·4244
	9	0	0·4324	*	0·4423
			neck		
	32	45	0·0568	0·0301	0·0458
	36	45	0·0501	0·0247	0·0393
	40	45	0·0456	0·0218	0·0357
	44	45	0·0428	0·0202	0·0334
	48	45	0·0412	0·0193	0·0321
	52	45	0·0404	0·0188	0·0314
[111]	54·7	45	0·0402	0·0188	0·0313
	60	45	0·0408	0·0191	0·0318
	64	45	0·0421	0·0198	0·0328
	68	45	0·0444	0·0211	0·0347
	72	45	0·0480	0·0223	0·0376
			six-cornered rosette		
[111]	54·7	45	1·8144	1·8055	1·7933

* Indicates an orbit which is probably extended; i.e. its 'cyclotron mass' as defined on p. 150 is large.

CYCLOTRON RESONANCE

The extremal cross-sectional areas of the Fermi surface $E(\mathbf{k}) = E_F$ are smaller by $(\partial A/\partial E)\,\delta E_F$ than those of a neighbouring surface $E(\mathbf{k}) = E_F + \delta E_F$, so that the differences in area are proportional to the cyclotron masses. At each point on the Fermi surface the distance between the surfaces is inversely proportional to the velocity. If the Fermi surface

is $W_F = W(\mathbf{k})$, the neighbouring surface may be expected to be $W_F + \delta W_F = W'(\mathbf{k})$, where $W'(\mathbf{k})$ is a Fourier series similar to $W(\mathbf{k})$ but with slightly different coefficients. The easiest way to fit such a neighbouring surface is to investigate the changes in the cross-sectional areas due to variation of W_F and each coefficient of $W(\mathbf{k})$ in turn. This is done in table 7 for a few directions in a (110) plane for Cu VI. The combination of changes in the coefficients, which gives area changes proportional to the observed cyclotron masses, will give the velocity distribution over the Fermi surface.

TABLE 6. VARIATION OF AREA IN UNITS OF A_s WITH k_H IN UNITS OF k_s FOR CU VI

	H in spherical polars		value of k_H, i.e. distance from symmetry plane				
	θ	ϕ	0	0·041	0·081	0·122	0·163
[100]	0	0	0·9700	0·9680	0·9620	0·9523	0·9397
	17	0	0·9709	0·9695	—	—	—
	21	45	0·9663	0·9660	—	—	—
[111]	54·7	45	0·9394	0·9395	0·9400	0·9411	0·9440
[110]	45	0	0·4063	0·4104	—	—	—
[100] rosette	0	0	0·4042	0·4081	—	—	—
[111] neck	54·7	45	0·0402	0·0414	—	—	—

TABLE 7. DIFFERENCES IN CENTRAL CROSS-SECTIONAL AREAS OF SURFACES BASED ON CU VI

angle from [001] in a (110) traverse	areas of Cu VI unaltered	differences between Cu VI and the surfaces with an increase of 0·002 in						cyclotron masses for copper
		W_F	C_{200}	C_{211}	C_{220}	C_{310}	C_{321}	
0°	0·9709	0·0014	−0·0031	−0·0051	−0·0040	−0·0033	−0·0081	1·385
6°	0·9689	0·0014	−0·0028	−0·0050	−0·0041	−0·0032	−0·0081	1·35
8°	0·9678	0·0014	−0·0035	−0·0050	−0·0041	−0·0032	−0·0081	1·31
10°	0·9667	0·0014	−0·0036	−0·0050	−0·0042	−0·0031	−0·0081	1·30
20°	0·9661	0·0017	−0·0057	−0·0055	−0·0046	−0·0035	−0·0094	1·37
54·7°	0·9398	0·0018	−0·0078	−0·0054	−0·0055	−0·0045	−0·0110	1·355
90°	0·4062	−0·0022	0·0097	0·0069	0·0044	0·0045	0·0054	1·23
neck area	0·0402	0·0014	−0·0082	−0·0042	−0·0012	−0·0035	−0·0095	0·6

The cyclotron mass figures (in units of the free electron mass) are taken from Kip *et al.* (1961). The slight discrepancies between column 2 of this table and column 5 of table 5 are due to the smaller step-length used in this table.

It may be noticed in passing that since table 7 indicates, for a typical case, the sensitivity of the cross-sectional areas to changes of the individual coefficients, it is also useful in showing what changes of coefficients would be required to modify the Fermi surface if future experiments of higher accuracy should suggest slightly different values of de Haas–van Alphen frequencies.

The only experimental information on the variation of cyclotron mass with field direction for these metals is that of Kip *et al.* (1961) for copper in the (110) plane. Their results are shown in figure 4, together with the variation in cross-sectional area of Cu VI, which is, of course, the same as the variation of de Haas–van Alphen frequency (see figure 7 of I, which does not, however, include the dog's bone).

Both area and mass are properties of the orbit considered, but it can be seen that, in spite of this, there is only a very rough similarity between the general behaviour of the

curves. Both should show discontinuities when the nature of the orbit changes (e.g. from round one belly to round three, or from electron- to hole-type). Now the nature of the orbit changes when the orbit slides off the neck, and this is largely determined by the size of the neck; the shape of the surface elsewhere is not of great importance. The angles at which these changes occur, calculated from the neck-size observed by Shoenberg,* are 25°, 46°, and 72°, and these are consistent with the computed Cu VI area curve and with

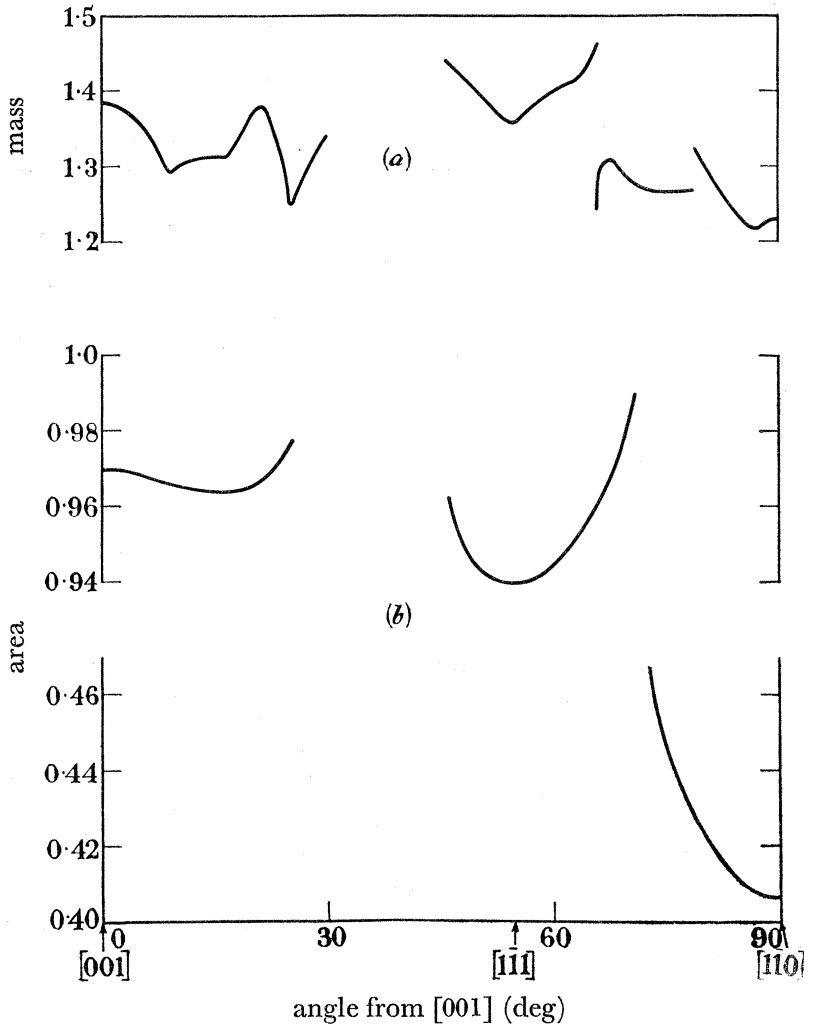

FIGURE 4. (*a*) Experimental cyclotron masses (Kip *et al.* 1961) and (*b*) theoretical (Cu VI) central cross-sectional areas for copper for magnetic field directions in a (110) plane. Note the different scales for mass and area.

the experimental observations on magneto-resistance (Alekseevski & Gaidukov 1959, interpreted by Priestley 1960). Even if the neck-size were wrong by 10%, the limiting angles would change by only one or two degrees. As can be seen from figure 4, the discontinuities in the mass curve occur at 30°, 46°, 66°, and 79°, only one of which agrees with the limiting angles derived from the Fermi surface.

* For copper the limiting angles could not be directly observed in measurements of the de Haas–van Alphen effect, but for silver and gold direct observation of the limiting angles was possible and, as can be seen from figures 8 and 10 of I, they agree to within 1 or 2° with those computed from the fitted Fermi surfaces.

The discrepancies may be due to the difficulties of interpreting the cyclotron resonance experiments, and indeed Kip *et al.* themselves express doubt about the correct interpretation between 25° and 30°, and between 66° and 79°. Moreover, since the mass is proportional to $\partial A/\partial E$, it must become infinite when an orbit slides off a neck, so that the mass discontinuities at 66° and 79° shown in figure 4 are not plausible physically. (The areas do not and should not increase without limit at the limiting angles.)

The disappearance of the experimental signal is to be expected before a limiting angle is reached, both for the mass and the de Haas–van Alphen effect, because they vary rapidly both with angle and with k_H, the component of **k** parallel to **H**, so that the amplitude falls off rapidly. If we consider the mass curve between 0° and 30° and reject the portion between 25° and 30° (because it goes beyond the limiting angle indicated by the neck-size and because of the doubts expressed by Kip *et al.*), we should also reject the portion between 22° and 25°, because of its downward slope which gives an unplausible mass at the limiting angle (25°). In place of the regions between 22° and 30° and between 66° and 79° (which we also reject because of the wrong mass discontinuities and the doubts of Kip *et al.*), we would expect the mass curve to continue upwards from 22° to an infinite value at about 25°, and have similar extensions from 66° to 72°, and from 79° to 72°.

Because of these doubts, we shall use for our calculations a few representative points which describe the behaviour of the curve between 0° and 22°, and the mass values at [111] (54·7°) and [110] (90°) and the neck. The mass values for seven field directions and the neck are given in column 9 of table 7. The entries in columns 3 to 8 are 0·002 times $(\partial A/\partial W_F)$, $(\partial A/\partial C_{200})$, etc., and we can then construct nine simultaneous equations of the form

$$m_r = \left(\frac{\partial A}{\partial W_F}\right)_r \delta W_F + \left(\frac{\partial A}{\partial C_{200}}\right)_r \delta C_{200} + \ldots + \left(\frac{\partial A}{\partial C_{321}}\right)_r \delta C_{321}$$

for the six unknowns δW_F, δC_{200}, ..., δC_{321}, whose ratios we wish to know.

Unfortunately, these equations turn out to be inconsistent, even if we reject the neck mass, which is less reliable than the others. The trouble is that the dip in mass at 9° is too deep and too close to [100]. With extra terms in the Fourier expansion, it might be possible to fit the experimental mass curve where it is plausible, but with a six-term series the experimental mass cannot be fitted, even after rejecting the more dubious experimental points. Thus the velocity distribution remains unknown.

Possibly the basic cause of the trouble is that the mass measured in the cyclotron resonance experiments is not exactly $\partial A/\partial E$ for the extremal cross-section, but a weighted average over k_H (see also I, p. 114). Although the difference between the measured mass and the mass characteristic of the extremal cross-section may not be large (calculations of Kip *et al.* suggest that a difference of a few parts per cent is not unlikely), the difference may be strongly orientation-dependent. Since it is essentially the orientation dependence of mass which is involved in the above attempted calculations of an energy surface neighbouring to the Fermi surface, it is not too surprising perhaps that it is impossible to find a consistent solution, which would give the velocity distribution over the Fermi surface. If this is indeed the trouble, it may be noted that it could be eliminated by using cyclotron masses derived from the temperature variation of the de Haas–van Alphen

effect (where, because of the much higher phase of the oscillations, only the extremal value of $\partial A/\partial E$ is measured; see I, p. 114). As pointed out in I (p. 111), this would involve tedious experiments and, moreover, the experimental technique would require considerable improvement to achieve the necessary precision.

I wish to thank the Department of Scientific and Industrial Research for a research maintenance grant during the major portion of this work.

It is impossible to over-estimate the contribution of Dr D. Shoenberg, F.R.S., to this paper. He provided the initial impetus and has removed as many flaws as I would let him from the final form of the presentation. My supervisor, Dr J. M. Ziman, who first introduced me to electronic transport theory, and Professor A. B. Pippard, F.R.S., have explained a great deal of physics to me. I have been very fortunate in this, and am most grateful to them both. I also wish to thank most of the solid-state physicists in the department for valuable discussions.

I am also very grateful to Mr E. N. Mutch and the staff of the Cambridge University Mathematical Laboratory for the generous provision of time and priority on EDSAC II. I wish to thank Mr P. L. Taylor and Mr B. R. Austin for acting as intermediaries between me and the machine while I have been in Oxford; they have both wasted a great deal of time through my mistakes.

I am very grateful to Professor R. W. Morse, Professor A. F. Kip, Professor H. V. Bohm, Dr T. W. Moore, Dr B. Segall and Dr V. M. Morton for permission to reproduce published and unpublished experimental and theoretical results, and for discussing them with me.

References

Alekseevski, N. E. & Gaidukov, Yu. P. 1959 *J. Exp. Theor. Phys. U.S.S.R.* **37**, 672 (*Sov. Phys.* **10**, 481).
Bohm, H. V. & Easterling, V. J. 1962 *Phys. Rev.* (to be published).
Burdick, G. A. 1961 *Phys. Rev. Lett.* **7**, 156.
Chambers, R. G. 1952 *Proc. Roy. Soc.* A, **215**, 481.
Cornwell, J. F. 1961 *Phil. Mag.* **6**, 727.
García Moliner, F. 1958 *Phil. Mag.* **3**, 207.
Gold, A. V. 1958 *Phil. Trans.* A, **251**, 85.
Hume-Rothery, W. & Roaf, D. J. 1961 *Phil. Mag.* **6**, 55.
Kip, A. F., Langenberg, D. N. & Moore, T. W. 1961 *Phys. Rev.* **124**, 359.
Morse, R. W., Myers, A. & Walker, C. T. 1961 *J. Acoust. Soc. Amer.* **33**, 699.
Morton, V. M. 1960 Ph.D. Thesis Cambridge University.
Pippard, A. B. 1957 *Phil. Trans.* A, **250**, 325.
Priestley, M. G. 1960 *Phil. Mag.* **5**, 111.
Segall, B. 1962 *Phys. Rev.* **125**, 109.
Shockley, W. 1950 *Phys. Rev.* **79**, 191.
Slater, J. C. & Koster, G. F. 1954 *Phys. Rev.* **94**, 1498.
Ziman, J. M. 1960 *Electrons and phonons* §12.7. Oxford University Press.
Ziman, J. M. 1961 *Advanc. Phys.* **10**, 1.

PHILOSOPHICAL TRANSACTIONS OF THE ROYAL SOCIETY A MATHEMATICAL, PHYSICAL & ENGINEERING SCIENCES

Appendix. Numerical calculations

Details of integration

Various integrals are required over parts of the whole of the Fermi surface. For the magneto-resistance the integral has to be performed over the whole life-history of each electron (Shockley 1950; Ziman 1960) and Ziman suggested using this life-history to scan the surface. Thus, an electron with momentum $\hbar\mathbf{k}$ and velocity $\mathbf{v}$ will move in a magnetic field $\mathbf{H}$ in such a way that $\hbar\dot{\mathbf{k}} = e(\mathbf{v}\times\mathbf{H})/c$; consequently successive values of $\mathbf{k}$ are given by integrating $(\mathbf{v}\times\mathbf{H})$ with respect to time. Numerically this means taking $\mathbf{k}+e(\mathbf{v}\times\mathbf{H})\delta t/c\hbar$ as the next value of $\mathbf{k}$.

If the electron is at point $\mathbf{k}$ on the Fermi surface at any time, it will remain there subsequently since $\mathbf{v}$ (which is $\mathrm{grad}_{\mathbf{k}}E/\hbar$, where E is the energy) is normal to the surface, so that $\dot{\mathbf{k}}$, which is normal to $\mathbf{v}$ and $\mathbf{H}$, lies in the surface. Thus the successive values of $\mathbf{k}$, passed through in the course of integration with respect to time, define a cross-section of the surface with a constant component, k_H, of $\mathbf{k}$ parallel to $\mathbf{H}$.

To check that a point $\mathbf{k}$ is on the Fermi surface, it is only necessary to calculate $E(\mathbf{k})$ and confirm that it is, within a specified small tolerance, equal to E_F, the Fermi energy. If it is not, replacement of $\mathbf{k}$ by

$$\mathbf{k}+\frac{[E_F-E(\mathbf{k})]\ [H^2\mathbf{v}-(\mathbf{v}.\mathbf{H})\mathbf{H}]}{[H^2v^2-(\mathbf{v}.\mathbf{H})^2]\hbar},$$

gives, by Newton's method, a point with the same value of k_H, which should be a better approximation; thus we have an iterative approach to the surface.

With a check to recognize the starting point, an orbit can be followed round the surface. The total time taken will be the cyclotron period, which is proportional to the cyclotron mass. If we now increase k_H, and move back on to the surface we can follow the electron's $\mathbf{k}$-trajectory on a new cross-section of the surface.

Some refinements are necessary to deal with surfaces which contact the zone-faces. Whether or not an orbit intersects a zone-face can be easily decided for an f.c.c. space-lattice (i.e. a b.c.c. reciprocal lattice) by computing $\frac{1}{2}a|k_x|$, $\frac{1}{2}a|k_y|$, and $\frac{1}{2}a|k_z|$ and testing whether each of these is less than π, and their sum less than $\frac{3}{2}\pi$. For some of the integrals only the values of $\mathbf{k}$ within the zone must be used and subroutines have been developed to move the value of $\mathbf{k}$ around the faces of the zone until another intersection is found. With these refinements, we have a procedure for scanning the surface.

It is possible to adjust this procedure so that we integrate over only a forty-eighth of the surface and obtain the remainder by symmetry transformations. This is all that is necessary for surface area, volume, density of states, and anomalous skin effect. For the magneto-resistance, integration is needed over the life-history of all electrons on one-half of the surface, while for the de Haas–van Alphen effect and cyclotron mass it is needed round the appropriate cross-section.

In fact *any* surface described by an implicit equation of the form $f(\mathbf{k}) =$ constant can be scanned in the way discussed above, if we take $E(\mathbf{k})$ as $f(\mathbf{k})$ and $\mathbf{v}$ as $(1/\hbar)\ \mathrm{grad}_{\mathbf{k}}\ f$; t is now an arbitrary variable, t and $\mathbf{v}$ are no longer to be identified with time and velocity although $\mathbf{v}$ will be parallel to the velocity since both are normal to the surface. (It will be

seen that only the direction of the normal is required for the scanning procedure above.) **H** is any vector in the direction of the magnetic field.

If $W_F = W(\mathbf{k})$ is a good approximation to the true surface, any integral which does not require the true magnitude of the velocity will be correct, even though $W(\mathbf{k})$ is a poor approximation to the true band-structure. Thus, the de Haas–van Alphen effect, the anomalous skin effect, the volume and the total surface area corresponding to $W_F = W(\mathbf{k})$ will be correctly computed, but the 'density of states', , the 'cyclotron masses', and the 'magneto-resistance', obtained by regarding $W_F = W(\mathbf{k})$ as if it were a true band-structure, will be wrong.

The 'cyclotron mass' would, in fact, be proportional to $\partial A/\partial W_F$, and for any particular field direction for Cu VI this is proportional to the entry in column 3 of table 7. It can be seen that the angular variation of these pseudo 'cyclotron masses' is not very similar to that of the experimentally determined masses of column 9.

The integrals over a forty-eighth of the surface (volume, surface area, and anomalous skin effect) involve integration over an element of surface area $\mathrm{d}S$. These were done as double integrals, replacing $\mathrm{d}S$ by $vH\mathrm{d}k\mathrm{d}k_H/[H^2v^2-(\mathbf{v}.\mathbf{H})^2]^{\frac{1}{2}}$, where $\mathrm{d}k$ and $\mathrm{d}k_H$ are the distances between successive points and between successive sections of the surface respectively. **H** was along [100], and the forty-eighth had corners at [111], [010], and [011] so that **v** would not be parallel to **H** at any point. Since $\mathrm{d}k_H$ was constant, the integrals reduced to single integrals over $\mathrm{d}k$, provided that points on the edges of the forty-eighth are weighted by a factor of one-half and the corners [111], [010], and [011] by one-sixth, one-eighth, and one-quarter, respectively. The integrals for the de Haas–van Alphen effect (extremal cross-sectional area) were single integrals over $\mathrm{d}k$.

The total surface area is given by $\int \mathrm{d}S$, the volume by $\frac{1}{3}\int \frac{\mathbf{k}.\mathbf{v}}{v}\mathrm{d}S$, and the cross-sectional area by $\frac{1}{2}\int \frac{\mathbf{H}.\mathbf{k}\times\mathrm{d}\mathbf{k}}{H}$.

The integral necessary for computing the magneto-resistance has been given by Ziman (1960) but, although this integration was performed for a few directions of **H**, on special assumptions about the electron velocities and relaxation times, the results will not be given here because they are not sufficient to give anything like a reliable overall picture. To provide a comprehensive survey would require integrations for many more directions of **H**, and would involve too much computing time. In any case a reasonable knowledge of electron velocities would be essential and, as discussed on p. 147, this is not available.

The integral for the anomalous skin effect is taken from Morton (1960) in which he justifies and improves on Pippard's 'ineffectiveness concept'. The integral finally arrived at is not very different from that used by Pippard (1957) for copper. The complex impedances Z_x, Z_y in the two directions in the surface of the specimen are given by

$$Z_{x,y} = \frac{4}{3\sqrt{3}}\left[\frac{2\pi^2\omega^2}{(A_{x,y})}\right]^{\frac{1}{3}}(1+\sqrt{3}\,\mathrm{i}),$$

where ω is the applied angular frequency and

$$A_{x,y} = \frac{e^2}{4\pi^3\hbar}\epsilon\int \frac{n_{x,y}^2\,\mathrm{d}S}{\cos^2\theta+\epsilon^2},$$

where ϵ is a constant, $\mathbf{n}$ is a unit vector in the direction of the velocity, θ is the angle between the normal to the specimen surface and the velocity, and the integration is performed over the Fermi surface (dS being an element of surface area). The exact value of ϵ is not very important; Morton estimated it at 0·0306 for silver and this value has been used for copper as well in these calculations. It measures, in a sense, the ineffectiveness angle which is here taken as $1\frac{3}{4}°$. The observed surface resistances, R_x and R_y, referred to in table 2 and figure 2, are the real parts of Z_x and Z_y. The anomalous skin effect experiments were performed on a number of specimens, the normals to whose surfaces lay approximately in a (110) or (100) plane and R_y was measured along [110] or [100], respectively, while R_x was measured perpendicular to R_y.

Accuracy

No point was allowed to be more than $10^{-4}k_s$ from the surface (in the plane of constant k_H), where k_s is the radius of the Fermi sphere ($\frac{1}{2}ak_s = 2{\cdot}456$, where a is the lattice spacing—see table 2 of I). The step-length for the de Haas–van Alphen effect (i.e. for extremal areas) was normally between 5 and $7\times10^{-2}k_s$, but the steps, being proportional to $\mathrm{grad}_k W$, are smaller in general in regions of high curvature so that the necks are scanned more closely than the bellies, which improves the accuracy. Since areas are computed from the inscribed polygon they are slightly lower than the true values; the deficiency is between 4 and $8\times10^{-4}\,A_s$ for the nearly circular belly orbits where $A_s(=\pi k_s^2)$ is the extremal area of the Fermi sphere. No correction has been made for this deficiency in tables 5 and 7* (or in the graphs shown in I), because the variation in step-length (due to variation in $\mathrm{grad}_{\mathbf{k}}W$) is indeterminate, and the correction, therefore, is uncertain, and because, as far as fitting is concerned, only differences in area are involved and the corrections are always in the same sense and approximately equal, so that these inaccuracies are normally well within the error of the experiments.

It is difficult to estimate the accuracy of computation of the anomalous skin effect. Normally the integration was over 250 points in one forty-eighth of the surface, which represents a 2° mesh. With $\epsilon = 1\frac{3}{4}°$, this should not lead to much inaccuracy unless the surface is badly corrugated, but a trial was made for the García Moliner (1958) surface with a closer mesh over 1500 points in a forty-eighth of the surface, representing some seventy thousand points on the whole surface, and the differences in the anomalous skin effect were nowhere more than 1%. As can be seen from the graphs (figure 2), such small differences are hardly significant.

Volumes and surface areas should be accurate to 0·1% and all the new theoretical surfaces in table 1 have computed volumes of one electron per atom to this accuracy.

Fitting procedure

The necks of all the theoretical surfaces are almost circular, so that all surfaces through a point on the (111) hexagonal zone-face have the same neck area. With a given value for N (see equation (2)), a point on the neck is easily found, and the values of the separate terms in the Fourier series (equation (1)) can be calculated. Thus, with given values of the coefficients of $W(\mathbf{k})$, the value of W_F corresponding to a surface through the point on

* The step-length has, however, been halved in table 7 to improve the accuracy.

the neck is given by substituting in equation (1). The values of D, D_1 (D_2 for gold) (see (2)), and the volume V, could then be computed for this surface. If these values differed from the desired values the calculations were repeated for three further surfaces in which all the coefficients of $W(\mathbf{k})$ except, in turn, C_{200}, C_{220}, and C_{310}, were kept constant; one of these three was varied slightly, and W_F was adjusted to keep the neck-size equal to the experimental value of N. (Some idea of the dependence of area on the various parameters in (1) can be deduced from table 7, although there the neck-size has not been kept constant.) From the values of D, D_1 or D_2, and V, for the four slightly different theoretical surfaces, we immediately obtain (to a first-order approximation) values of $(\partial D/\partial C)$, $(\partial D_1/\partial C)$ or $(\partial D_2/\partial C)$, and $(\partial V/\partial C)$, where C represents, in turn, C_{200}, C_{220}, and C_{310}. The changes δC_{200}, δC_{220}, and δC_{310} in the coefficients needed to bring D, D_1 or D_2, and V to their desired values, are now easily obtained from the solution of the three simultaneous equations of the form

$$\frac{\partial D}{\partial C_{200}}\delta C_{200}+\frac{\partial D}{\partial C_{220}}\delta C_{220}+\frac{\partial D}{\partial C_{310}}\delta C_{310} = \text{desired change in } D.$$

W_F is then adjusted to keep the neck-size correct. Since this procedure neglects second-order changes it is usually necessary to repeat the procedure until the desired values of D, D_1 or D_2, and V are obtained with the requisite accuracy.

This fitting procedure was used to derive the parameters of the four-term surfaces Cu IV, Ag IV, and Au IV (in which, of course, $C_{211} = C_{321} = 0$). The five-term gold surface Au V was found by taking arbitrary values of C_{321}, re-adjusting the other coefficients (with $C_{211} = 0$) to give the correct values for D, D_2, and the volume, calculating D_1, and choosing the value of C_{321} which gave the correct value for D_1. The six-term surfaces Cu VI and Ag VI were found in a similar way, the coefficients C_{211} and C_{321} being chosen by interpolation to give the best fit with the anomalous skin effect. This procedure was not, perhaps, the ideal one and, if it had been realized initially that some three hundred surfaces would be investigated, more sophisticated techniques might have been used.

Further comments on the computer program

The program, written in the one-address machine code for EDSAC II, contains some 2500 instructions. Any implicit equation of the form $f(\mathbf{k}) = \text{constant}$, with less than seven parameters can be used (the only two used so far have been the polynomials of Pippard (1957) and Morton (1960) and the Fourier series $W_F = W(\mathbf{k})$). The program is not restricted to dealing with cubic symmetry, and can also deal with surfaces of more than one sheet.

PHILOSOPHICAL TRANSACTIONS OF THE ROYAL SOCIETY A MATHEMATICAL, PHYSICAL & ENGINEERING SCIENCES